

Optical properties of subwavelength hole arrays in vanadium dioxide thin films

E. U. Donev,* J. Y. Suh, F. Villegas, R. Lopez, R. F. Haglund, Jr., and L. C. Feldman
Department of Physics and Astronomy, Vanderbilt University, Nashville, Tennessee 37235, USA
and Vanderbilt Institute of Nanoscale Science and Engineering, Nashville, Tennessee 37235, USA

(Received 13 April 2006; published 16 May 2006)

We demonstrate that the transmission of far- and near-field incident light through a periodic array of subwavelength holes in a vanadium-dioxide (VO_2) thin film is enhanced in the infrared range with respect to transmission through the unperforated film when VO_2 undergoes its semiconductor-to-metal transition. We explain this enhancement by analyzing the loss of transmitted intensity due to leaky evanescent waves inside the holes and scattering at the entrance and exit apertures. Numerical simulations based on the transfer-matrix formalism provide qualitative support for the model and reproduce the principal features of the experimental measurements.

DOI: [10.1103/PhysRevB.73.201401](https://doi.org/10.1103/PhysRevB.73.201401)

PACS number(s): 78.67.-n, 42.25.Bs, 71.30.+h, 78.20.Bh

The optical properties of periodic arrays of subwavelength holes continue to excite intense interest among researchers, especially in regard to opaque metal films.¹⁻⁵ However, the transmission behavior of subwavelength holes within partially transparent films has, thus far, remained unexplored. In such systems, the overall transmission results from a competition between propagating and evanescent modes, whose interplay crucially depends on the boundary conditions at the interface between the holes and the semi-transparent host material. Through a combination of nanostructuring and an optical phase transformation, the present work investigates this interaction.

We report the observations of optical transmission through a periodic subwavelength hole array in a thin VO_2 film during its reversible semiconductor-to-metal transition. We compare the far-field transmission of the hole array to the transmission of a plain (unperforated) area of the film in each phase of the material. Particularly intriguing is the wavelength dependence of the transmission as the ratio of light detected from the hole array to that from the plain film *reverses* in the near-infrared (near-IR) range of metallic-phase VO_2 . Images obtained with near-field illumination visually reveal the source of this effect: The light emerging from each air-filled hole undergoes a different modulation depending on the phase of the surrounding VO_2 material and the incident wavelength.

These observations, in conjunction with numerical simulations, demonstrate that the different wavelength-dependent optical constants of the two VO_2 phases modify the hole-array transmission in a complex and subtle manner. We propose a heuristic model that captures the salient features of the observed transmission behavior. It accounts for intensity losses due to evanescent waves “leaking” into the VO_2 layer as well as diffuse light scattering from the entrance and exit apertures. The role of the inner interface of each hole manifests itself in the wavelength dependence of the dielectric contrast between air and VO_2 , especially so in the metallic phase of the material.

The experiments make use of the phase-dependent optical properties of VO_2 .⁶ The phase transition in VO_2 occurs at a critical temperature $T_c \approx 67^\circ\text{C}$, from a high-temperature, rutile, metallic phase to a low-temperature, monoclinic, semiconducting phase.⁷ Below T_c , the unperforated film is

considerably *more* infrared transparent than it is in the metallic phase (above T_c). Remarkably, the transition can take place in less than 100 fs when induced by a laser pulse.⁸ The VO_2 layer in our experimental structure was fabricated on a fused-silica substrate, in a pulsed-laser deposition system (KrF excimer: $\lambda = 248$ nm), by ablating a vanadium target in a 12-mTorr O_2 atmosphere at 550°C . The resulting film thickness was 200 nm, as determined by Rutherford backscattering spectrometry. The hole array was milled down to the substrate with a focused-ion beam (FIB) system (30-keV Ga^+ ions). Figure 1(a) shows the FIB micrograph of a hole array in VO_2 ; the geometrical parameters are given in the caption of Fig. 1(b). The crucial control parameter was the change in the optical constants of VO_2 during the thermally induced phase transition.

Spectral measurements at normal incidence were performed with collimated white light delivered through an optical fiber and a micro-objective [Fig. 1(c)]. The incident beam spot was slightly smaller than the size of the array, and beam divergence was determined to be $\pm 1^\circ$. Transmission spectra T_{00} , consisting of light emerging from the holes as well as from the unperforated interhole areas, were collected in the zero diffraction order (i.e., detected beam is collinear with the incident beam) by another micro-objective, stopped down to reduce outgoing-beam divergence to $\pm 1^\circ$, and coupled to a fiber. The fiber was fed into a monochromator equipped with a cooled charge-coupled-device (CCD) detector. The substrate was attached to a resistively heated sample holder, mounted on a translation-rotation stage, with a precision thermocouple placed in contact with the top surface of the sample. The position of the hole array was monitored in reflection via a CCD camera connected to a video display. A scanning near-field optical microscope (SNOM) setup [Fig. 1(d)] was used to image the far-field transmission through the holes under near-field illumination. The inset in Fig. 1(d) is a SNOM image of perforated semiconducting-phase VO_2 .

The experimental results presented in Figs. 2(a) and 2(b) show T_{00} spectra of plain and perforated VO_2 in each phase of the material. Both the reflected (R_{scatt}) and the transmitted (T_{scatt}) scattering propagate out of the detector path and consequently do not contribute to T_{00} . In addition, a portion of the diffracted field travels through the subwavelength holes

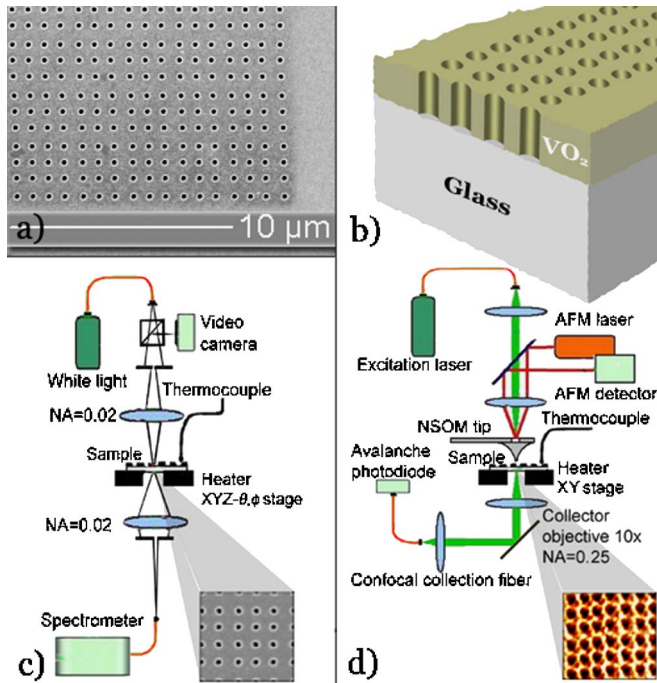


FIG. 1. (Color online) (a) FIB micrograph and (b) schematic of a section of a hole array in VO_2 on glass (60×60 holes, diameter = 250 nm, pitch = 750 nm, film thickness = 200 nm). (c) Schematic of the optical setup used for spectral measurements. (d) Schematic of the SNOM setup used to obtain the images in Fig. 3 and this (inset) image of semiconducting-phase, visible-light ($\lambda = 532$ nm) transmission.

as “leaky waves,” that is, evanescent waves that lose intensity as they propagate along the holes.⁹ The VO_2 material surrounding the holes acts as a lossy medium: The waves penetrate the side walls of the holes and “leak” into the plane of the VO_2 layer, where absorption (I_{absorb}) occurs. As a result, even more of the incident light is diverted away from the normal path and rendered undetected in the far field.

Figure 2(a) compares the semiconducting-phase T_{00} through the hole array and through the unperforated area. Overall, the hole array transmits less than the intact film in this phase. This occurs partly because the array and each aperture serve as a diffraction grating and an individual scatterer, diverting some of the incident light into nonzero diffracted orders and diffuse scattering, respectively, and also because the leaky waves lead to further intensity losses. Therefore, direct transmission through the partially transparent VO_2 film overwhelms the light emerging from the holes, so that the exit apertures appear darker than their surroundings in the above-mentioned SNOM image of the VO_2 array in the semiconducting phase [inset in Fig. 1(d)]:

However, Fig. 2(b) reveals an unexpected transmission trend in the near-IR region of the metallic-phase hole array: In spite of intensity losses due to diffraction (scattering) and leaky waves, T_{00} of the array exceeds T_{00} through the plain film (i.e., direct transmission). This subtle and intriguing observation warrants further exploration of the optical behavior of our perforated VO_2 .

Additional insight can be acquired through numerical calculations of the relevant optical quantities for perforated and

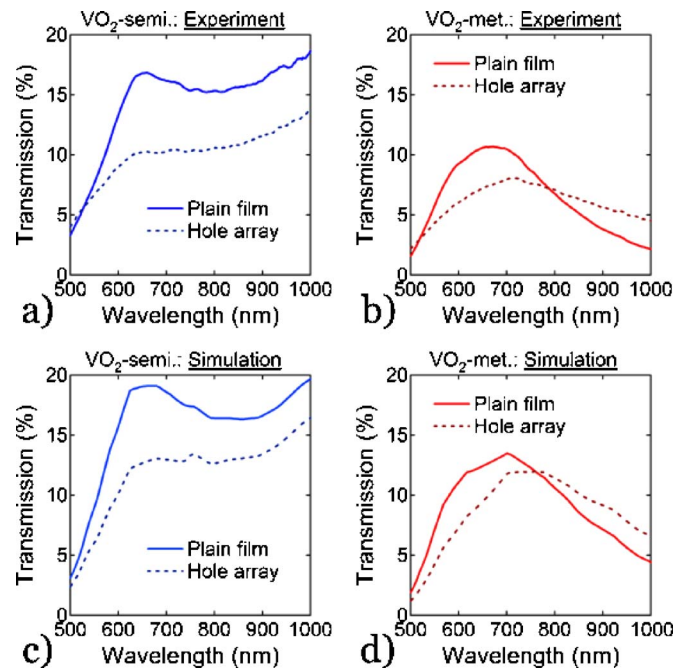


FIG. 2. (Color online) (a) and (b) Experimental and (c) and (d) simulated spectra of far-field, zero-order transmission T_{00} through perforated (dashed lines) and plain (solid lines) VO_2 films, obtained under far-field illumination during (a) and (c) semiconducting and (b) and (d) metallic phases. The optical constants of VO_2 were extracted from Ref. 6.

plain VO_2 films [Figs. 2(c) and 2(d)]. Our simulations are based on a numerical method for modeling the properties of patterned photonic crystal slabs.¹⁰ Maxwell’s equations are solved as an eigenvalue problem via plane-wave decomposition in two-dimensional Cartesian coordinates, and the solution is propagated across the different layers by means of transfer matrices, which define the continuity conditions for electromagnetic field components at an interface. The in-plane periodicity of the structure is represented by the Fourier transform of the piecewise dielectric permittivity. Despite some limitations, such as square instead of circular apertures, our simulations give semiquantitative agreement with the experimental data. In particular, the calculated curves for the metallic phase [Fig. 2(d)] show the most important feature: the characteristic crossover in the near-IR region, where the hole array transmits more than the plain film.

These results suggest a model, whereby the relative loss of transmitted intensity through the hole array depends on the dielectric permittivity (ϵ) contrast between the air-filled hole content and its surroundings (VO_2). Higher ϵ contrast increases both the scattering ($T_{\text{scatt}} + R_{\text{scatt}}$) from the apertures¹¹ and the leakage of evanescent waves⁹ into the VO_2 layer (part of I_{absorb}) [Fig. 3(a)]. Conversely, lower ϵ contrast reduces those losses [Fig. 3(b)]. Therefore, when surrounded by a material of similar real-part ϵ , i.e., metallic VO_2 in the near-IR, the air-filled holes act in favor of T_{00} by minimizing the undetected components of the total optical field. Furthermore, in comparison with the plain film, the hole array experiences smaller specular reflection (R_{00}) and

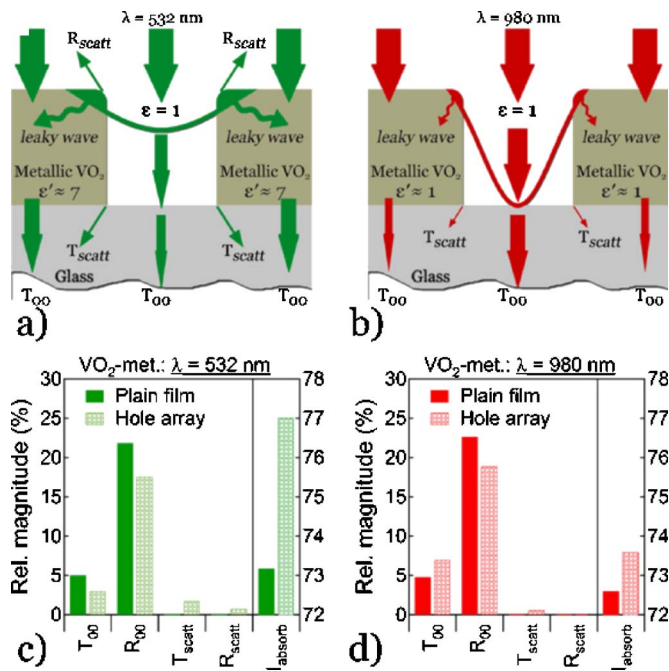


FIG. 3. (Color online) Schematics of light transmission through perforated metallic-phase VO₂ film: (a) visible and (b) near-IR wavelength. Simulated optical quantities for perforated (hatched bars) and plain (solid bars) metallic-phase VO₂ film: (c) visible and (d) near-IR wavelengths. According to our model, the lower dielectric contrast between the interior (air, $\epsilon=1$) and exterior ($\epsilon' \approx 1$; from Ref. 6) of each hole for metallic VO₂ in the near-IR reduces the losses from leaky-waves absorption (part of I_{absorb}) and diffuse scattering ($T_{scatt}+R_{scatt}$), to the extent that T_{00} through the array exceeds T_{00} through the film (direct transmission). Legend: T_{00} = zero-order transmission; R_{00} = specular reflection; T_{scatt} = forward diffuse scattering; R_{scatt} = backward diffuse scattering; I_{absorb} = absorption (right-side scale) = $100\% - T_{00} - R_{00} - T_{scatt} - R_{scatt}$.

direct absorption (the rest of I_{absorb}) in either phase, since a portion of the incident light encounters apertures instead of VO₂ material. Ultimately, when the scattering and absorption losses for the hole array have decreased enough with respect to those for the plain film, T_{00} through the array becomes larger than the direct transmission through the plain film.

The above analysis is borne out by previous measurements of the optical constants of VO₂.⁶ The complex permittivities of the two phases of VO₂ exhibit similar trends and values in the visible range, with the real parts trending away from 1 (air). In the IR range, however, these two permittivities differ significantly. Because of the decreased ϵ contrast between the interior (air) and exterior VO₂ of the holes in the case of metallic VO₂ at IR wavelengths [Fig. 3(b)], T_{00} through the hole array prevails over T_{00} through the intact film, hence the unexpected crossover in Fig. 2(b).

The relative magnitudes of T_{00} , R_{00} , T_{scatt} , R_{scatt} , and I_{absorb} (right-side scale) are charted in Figs. 3(c) and 3(d) for plain and perforated VO₂ in the metallic phase, each at two different wavelengths. As noted earlier, R_{00} for the plain film is considerably greater than R_{00} for the hole array. Conversely, I_{absorb} for the array is appreciably greater than I_{absorb} for the plain film at the visible wavelength [Fig. 3(c)], while at the near-IR wavelength [Fig. 3(d)], the two absorptions are almost equal because the effect of the leaky waves is minimized. In the latter case, since the plain film reflects specularly (R_{00}) more than the hole array, and since the total diffuse scattering of the array is rather small (T_{scatt} only, as $R_{scatt}=0$ for $\lambda \geq 750$ nm), conservation of energy requires that the hole array transmit *more* in the zero order (T_{00}) than the plain film [Fig. 3(d)].

Perhaps most revealing of all are the SNOM image scans of far-field transmission through individual holes as well as unperforated areas, obtained under near-field incident illumination with green and near-IR laser light (Fig. 4). Below each image is a plot of the detected intensity along part of a row of apertures and extending outside the array into the plain film. The relative position of the rightmost aperture is marked by an arrow in each plot. In semiconducting VO₂ [Figs. 4(a) and 4(c)], the intensity reaches the local minima within the apertures relative to the film, indicating a leakage path through the film at both wavelengths. These observations corroborate the spectral measurements and simulations of T_{00} for semiconducting VO₂ [Figs. 2(a) and 2(c)] by demonstrating that the air-filled holes transmit *less* than the plain film for both visible and near-IR illumination.

For metallic VO₂, the holes still transmit less than the surrounding film, *but* only with visible-light illumination

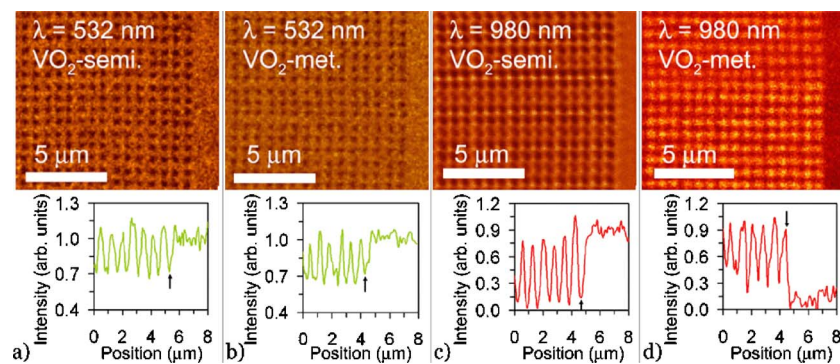


FIG. 4. (Color online) (Top half) SNOM images of far-field transmission through the VO₂ hole array, obtained with near-field illumination: (a) and (b) visible and (c) and (d) near-IR wavelengths, during (a) and (c) semiconducting and (b) and (d) metallic phases. (Bottom half) For each image above, intensity is plotted as a function of position along part of a row of holes and extending into the unperforated area outside of the array; the rightmost hole is indicated by an arrow in each plot.

[Fig. 4(b)]. In the near-IR range, however, the intensity contrast is reversed, so that more light emerges from each hole than from an equal-area spot on the intact film [Fig. 4(d)]. The overall effect of this behavior manifests itself in the transmission spectra for metallic-phase VO₂ [Figs. 2(a) and 2(d)], where the crossover in the near-IR signifies that T_{00} through the hole array exceeds the direct transmission through an unperforated area of the film. Once again, our model attributes this reversal to the *reduction of losses* from diffuse scattering, higher-order diffraction, and leaky waves for the metallic phase at near-IR wavelengths [cf., Figs. 3(a) and 3(b)] by virtue of the lower ϵ contrast between VO₂ and air.

To summarize: The present work deals with a previously unexplored aspect of light transmission through subwavelength hole arrays, namely, the interaction of the optical field inside the holes with the matrix of semitransparent material. For hole arrays in metallic VO₂, we observe a marked reduction of transmission losses in the near-IR ranges and attribute this effect to the diminishing permittivity contrast at the air-VO₂ interface inside the holes, brought about by the semiconductor-to-metal transition of VO₂.

VO₂-based hole-array structures also present a possible avenue for the development of new photonic devices. The intrinsic speed of the phase transition makes VO₂ a candidate for applications in fast optical switching,⁸ while the thermal hysteresis, especially prominent in nanoscale structures,^{12,13} may enable applications in memory and optical data storage.¹⁴ Moreover, the phase transition provides a novel way to modulate the anomalous transmission properties of subwavelength hole arrays in opaque metal films atop perforated VO₂ layers. Such double-layer structures greatly enhance the counterintuitive near-IR behavior of VO₂ described here, to the extent that the far-field transmission in the metallic phase actually exceeds its semiconducting counterpart.¹⁵

We thank A. B. Hmelo for helpful discussions on FIB fabrication, P. B. Gray for assistance with SNOM imaging, and N. L. Davis for creating Fig. 1(b). This research has been supported by the NSF Nanoscale Integrated Research Team (NIRT) program (DMR-0210785) and by a Major Research Instrumentation Grant (DMR-9871234).

*Electronic address: eugene.donev@vanderbilt.edu

¹T. W. Ebbesen, H. J. Lezec, H. F. Ghaemi, T. Thio, and P. A. Wolff, *Nature (London)* **391**, 667 (1998).

²L. Martin-Moreno, F. J. Garcia-Vidal, H. J. Lezec, K. M. Pellerin, T. Thio, J. B. Pendry, and T. W. Ebbesen, *Phys. Rev. Lett.* **86**, 1114 (2001).

³A. V. Zayats, L. Salomon, and F. de Fornel, *J. Microsc.* **210**, 344 (2003).

⁴H. J. Lezec and T. Thio, *Opt. Express* **12**, 3629 (2004).

⁵M. Sarrazin and J. P. Vigneron, *Phys. Rev. B* **71**, 075404 (2005).

⁶H. W. Verleur, A. S. Barker, and C. N. Berglund, *Phys. Rev.* **172**, 788 (1968).

⁷J. B. Goodenough, *J. Solid State Chem.* **3**, 490 (1971).

⁸M. Rini, A. Cavalleri, R. W. Schoenlein, R. Lopez, L. C. Feldman, R. F. Haglund, Jr., L. A. Boatner, and T. E. Haynes, *Opt.*

Lett. **30**, 558 (2005).

⁹K. Iizuka, *Elements of Photonics* (Wiley, New York, 2002).

¹⁰S. G. Tikhodeev, A. L. Yablonskii, E. A. Muljarov, N. A. Gippius, and T. Ishihara, *Phys. Rev. B* **66**, 045102 (2002).

¹¹W. Bogaerts, P. Bienstman, D. Taillaert, R. Baets, and D. De Zutter, *IEEE Photon. Technol. Lett.* **13**, 565 (2001).

¹²R. Lopez, L. A. Boatner, L. C. Feldman, R. F. Haglund, Jr., and T. E. Haynes, *Appl. Phys. Lett.* **79**, 3161 (2001).

¹³R. Lopez, L. C. Feldman, and R. F. Haglund, Jr., *Phys. Rev. Lett.* **93**, 177403 (2004).

¹⁴V. A. Klimov, I. O. Timofeeva, S. D. Khanin, E. B. Shadrin, A. V. Ilinskii, and F. Silva-Andrade, *Tech. Phys.* **47**, 1134 (2002).

¹⁵J. Y. Suh, E. U. Donev, R. Lopez, L. C. Feldman, and R. F. Haglund, Jr., *Appl. Phys. Lett.* **88**, 133115 (2006).